AD-777 685

THE DEPENDENCY OF COMPOSITE STRENGTH ON VOLUME FRACTION

M. J. Michno, Jr., et al

Monsanto Research Corporation

Prepared for:

Office of Naval Research
Advanced Projects Agency

March 1974

DISTRIBUTED BY:

NTIS

National Technical Information Service
U. S. DEPARTMENT OF COMMERCE
5285 Port Royal Road, Springfield Va. 22151

Security Classification

DOCUMENT CONTROL DATA - R & D AD 777 685

Security classification of title, body of abstract and indexing annotation must be entered when the overall report is classified)

1. ORIGINATING ACTIVITY (Corporate author)	2a. REPORT SECURITY CLASSIFICATION
Monsanto Research Corporation	Unclassified
	2b. GROUP

3. REPORT TITLE

The Dependency of Composite Strength on Volume Fraction

4. DESCRIPTIVE NOTES (Type of report and inclusive dates)

5. AUTHOR(S) (First name, middle initial, last name)

M. J. Michno, Jr. and E. M. Wu
R. E. Lavengood

6. REPORT DATE	7a. TOTAL NO. OF PAGES	7b. NO. OF REFS
March 1974		

8a. CONTRACT OR GRANT NO.	9a. ORIGINATOR'S REPORT NUMBER(S)
N00014-67-C-0218	HPC 73-156
b. PROJECT NO.	
c.	9b. OTHER REPORT NO(S) (Any other numbers that may be assigned this report)
d.	

10. DISTRIBUTION STATEMENT

Approved for public release: distribution unlimited

11. SUPPLEMENTARY NOTES	12. SPONSORING MILITARY ACTIVITY
	Office of Naval Research Washington, D. C.

13. ABSTRACT

The dependency of composite strength under combined normal stress has been experimentally determined as fiber content was varied over the range $40\% \leq v_f \leq 75\%$. Failure predictions of the tensor polynomial criterion agree well with experimental data in stress space. The maximum strain criterion predicts a physically inadmissible failure envelope in stress space due to the assumed linear constitutive law. In strain space the maximum strain criterion agrees favorably with experimental observation.

Reproduced by
NATIONAL TECHNICAL
INFORMATION SERVICE
U S Department of Commerce
Springfield VA 22151

I

DD FORM 1 NOV 65 1473 (PAGE 1)

S/N 0101-807-6801

Security Classification

14 KEY WORDS	LINK A		LINK B		LINK C	
	ROLE	WT	ROLE	WT	ROLE	WT
Strength						
Reinforced Plastics						
Volume Fracture						
Combined Stress						
Failure Criteria						
Tensor Polynomial						
Maximum Strain						

II

HPC 73-156

ITEM A002

THE DEPENDENCY OF COMPOSITE STRENGTH ON VOLUME FRACTION

by

M. J. Michno, Jr. and E. M. Wu
Washington University
St. Louis, Missouri 63130

and

R. E. Lavengood
Monsanto Company
Indian Orchard, Massachusetts 01051

March 1974

Monsanto/Washington University Association
High Performance Composites Program
Sponsored by ONR and ARPA
Contract No. N00014-67-C-0218, ARPA Order 876

Approved for Public Release: Distribution Unlimited

The views and conclusions contained in this document are those of the authors and should not be interpreted as necessarily representing the official policies either expressed or implied, of the Advanced Research Projects Agency or the U. S. Government.

III

FOREWARD

The research reported herein was conducted by the staff of Monsanto/Washington University Association under the sponsorship of the Advanced Research Projects Agency, Department of Defense, through a contract with the Office of Naval Research, N00014-67-C-0218 (formerly N00014-66-C-0045) ARPA Order No. 87, ONR contract authority NR 356-484/4-13-66, entitled "Development of High Performance Composites".

The prime contractor is Monsanto Research Corporation. The Program Manager is Dr. Rolf Buchdahl (Phone 314-694-4721).

The contract is funded for $7,000,000 and expires 30 June, 1974.

The Dependency of Composite Strength on Volume Fraction

by

M. J. Michno, Jr. and E. M. Wu
Washington University
St. Louis, Missouri 63130

and

R. E. Lavengood
Monsanto Company
Indian Orchard, Massachusetts 01051

Abstract

The dependency of composite strength under combined normal stress has been experimentally determined as fiber content was varied over the range $40\% \leq v_f \leq 75\%$. Failure predictions of the tensor polynomial criterion agree well with experimental data in stress space. The maximum strain criterion predicts a physically inadmissible failure envelope in stress space due to the assumed linear constitutive law. In strain space the maximum strain criterion agrees favorably with experimental observation.

The Dependency of Composite Strength on Volume Fraction

INTRODUCTION

Tsai and Wu [1] unified the treatment of composite material strength through a tensor polynomial approach. Specifically a general quadratic formulation was considered:

$$F_i\sigma_i + F_{i_j}\,\sigma_i\sigma_j = 1 \tag{1}$$

where in contracted notation

σ_i = stress tensor i = 1, ..., 6

F_i = strength tensors of 2nd order

F_{i_j} = strength tensors of 4th order

In general, equation (1) may represent a paraboloid, a hyperboloid, or an ellipsoid in the three dimensional stress space $(\sigma_1, \sigma_2, \sigma_6)$ characteristic of a general plane stress state. We rule out the possibility of infinite strength and hence require that:

$$F_{ii}F_{jj} - F_{ij}^2 > 0 \tag{2}$$

(no sum)

Thus equation (2) represents a stability condition in the sense that only ellipsoidal failure surfaces are admissible.

Expanding equation (1) taking account of symmetry results in the following expression restricted to plane stress states for orthotropic materials:

$$F_1\sigma_1 + F_2\sigma_2 + F_{11}\sigma_1^2 + F_{22}\sigma_2^2 + F_{66}\sigma_6^2 + 2F_{12}\sigma_1\sigma_2 = 1 \tag{3}$$

where $F_6 = F_{16} = F_{26} = 0$

Collins and Crane [2] discussed advantages of graphically representing the failure surface given by equation (3) in threee dimensions. This can be easily accomplished through computer graphics once appropriate solutions for the surface center, principal axes, and lengths of the semi-axes have been obtained from solid geometry. Knowledge of the size and shape of the failure surface in $(\sigma_1, \sigma_2, \sigma_6)$ space would allow prediction of failure for any stress state of interest including the various two-dimensional subspaces.

If we set shear stress $\sigma_6 = 0$ equation (3) represents an elliptical failure envelope in σ_1, σ_2 space (σ_1 = normal stress along the fiber, σ_2 = normal stress transverse to the fiber). Wu [3] has discussed in detail optimal experimental procedures for failure surface determinations in this stress space.

Herein the effect of constituent variables on composite strength will be determined. The primary emphasis will be on strength in σ_1, σ_2 space as fiber content is varied from 40 to 70 percent. However, shear strength determinations will be reported. The results of experiment will be compared to both the tensor polynomial strength criterion and the maximum strain failure criterion.

Specification of Failure Under Plane Normal Stress

The second and forth order strength tensors of equation (3) are related to engineering strengths in the following way [1]:

$$F_1 = \frac{1}{X} - \frac{1}{X'}, \quad F_{11} = \frac{1}{XX'}$$

$$F_2 = \frac{1}{Y} - \frac{1}{Y'}, \quad F_{22} = \frac{1}{YY'} \qquad (4)$$

$$F_{66} = \frac{1}{S^2}$$

F_{12} to be determined from combined stress tests

where X, X' = longitudinal tensile and compressive strength respectively

Y, Y' = transverse tensile and compressive strength respectively

S = shear strength

When $\sigma_6 \equiv 0$, the resulting elliptical failure surface in σ_1, σ_2 space is fully specified through knowledge of the strength tensors as follows [4]:

Center lies at; $-F_1/2F_{11}$, $-F_2/2F_{22}$

Major axis inclination wrt σ_1 axis;

$$\Theta = 1/2 \arctan F_{12}/F_{11} - F_{22} \qquad (5)$$

Semi-axes;
$$\frac{2}{F_{11} + F_{22} \pm \sqrt{(F_{11} - F_{22})^2 + 4F_{12}^2}}^{1/2}$$

Hence, we appeal to experimental results to effect the desired description of plane stress failure as a function of volume fraction.

Material and Specimens

Composites were prepared using the same materials and filament winding techniques reported in detail elsewhere [5]. All specimens were wound on steel mandrels (cylindrical for tubes, rectangular for plates) with Pittsburgh Plate Glass 1062-T6E glass fibers and Shell Epon 828 resin cured with 20 phr* curing agent Z. Volume fraction was controlled by varying the winding tension. After winding the specimens were vacuum impregnated at 60 to 70°C for 20 minutes to reduce voids. The mandrels were then rotated until the resin-gelled. The final cure was in a 150°C air circulating oven for 2 hours.

*phr = parts per hundred resin

Tubular samples were then ground to final dimensions. Finished tubes were 8 to 10 inches long with a mean diameter of 1 inch and a wall thickness of from 0.030 to 0.050 inches depending on volume fraction. Plate samples were cut into straight sided tensile specimens approximately 1/2 in. wide and 6 in. long with either longitudinal or transverse fiber direction. These were tabbed with glass fabric reinforced laminates to establish a gage length of 3 inches.

The fiber volume fractions were determined by burning broken samples and ranged from 38 to 76 percent. Void content of the samples was determined in accordance with ASTM Standard D2734-26. Results indicated that less than 1% voids were present.

Apparatus and Experimental Technique

The straight sided tensile specimens were tested in an Instron tester at a cross-head speed of 0.2 in/min. An extensometer was used to continuously record strains to compliment the continuous load record. All tests were conducted at room temperature ~75°F.

Tests on tubular samples were conducted on an MTS closed-loop servo controlled testing system. Experimental details are given in [3]. Continuous recordings of load were obtained for all specimens. In addition certain specimens were instrumented with electrical strain gage rosettes to allow monitoring of strain history. Applied loads were reduced to stresses based upon original cross sectional dimensions.

Test Results and Calculations

Uni-axial Normal Stress States

The determination of longitudinal and transverse tensile and compressive strengths as a function of volume fraction has been

reported elsewhere [6]. All strengths were found to vary in a linear fashion with volume fraction. Data analysis was carried out to arrive at a minimum root mean error through the least squares technique. The resulting expressions and the respective standards derivations are:

$$X = 225.49\ v_f + 6.86;\ S.D. = 10.59\ (ksi) \quad (6)$$

$$X' = 41.81\ v_f + 68.86;\ S.D. = 7.28\ (ksi) \quad (7)$$

$$Y = 5.64\ v_f + 4.13;\ S.D. = 0.95\ (ksi) \quad (8)$$

$$Y' = 15.74\ v_f + 13.71;\ S.D. = 1.64\ (ksi) \quad (9)$$

Knowledge of the functional dependency of X, X', Y, Y' on fiber volume and the defining equations (4) allows F_1F_2, F_{11}, and F_{22} to be calculated as a function of volume fraction. Results are shown in Figs. 1-4. In these figures the solid line represents the value of the strength tensor component while the dashed lines indicate plus and minus one standard deviation. The standard deviation was calculated from the appropriate standards deviations given in equations (6)-(9) and simple propagation of error theory [7] neglecting cross correlation terms.

Shear Stress State

For the sake of completeness the results of shear strength determinations [8] as a function of volume fraction for the 828Z-E glass system under study are reported. Shear strength (S) as determined by the short beam method (τ_{13}^{ult}) was found to fit:

$$S = -1.46\ v_f + 10.91;\ S.D. = 0.25\ (ksi) \quad (10)$$

$$38\% \leq v_f \leq 75\%$$

Shear strength (S) as determined by tube torsion tests (τ_{12}^{ult}) was found to fit:

$$S = -4.64\ v_f + 13.27;\ S.D. = 0.61\ (ksi) \qquad (11)$$

$$38 \leq v_f \leq 75\%$$

Generally in the range $38\% \leq v_f \leq 55\%$ the results of the short beam shear tests lie below the shear strength as determined by tube torsion. However, in the range $55\% \leq v_f \leq 75\%$ the two agree quite well.

The above results are recast into strength tensor form and shown in Fig. 5. Short beam shear results (Eq. 10) allow calculation of $F_{55} = \tau_{13}^{ult})^{-2}$ while the tube torsion results allow one to compute $F_{66} = (\tau_{12}^{ult})^{-2}$. F_{55} and F_{66} agree to within one standard deviation of F_{66} over the range $60\% \leq v_f \leq 75\%$.

Complex Stress States

The normal stress interaction strength tensor F_{12} must be determined from tests under a combined state of stress as described in [3]. Tests were conducted on hoop wound tubes subjected to combined axial load and interval pressure to produce various biaxial stress ratios $B = \sigma_1/\sigma_2$ for a range of volume fraction. Results are presented in Table 1.

The failure surface expressed in terms of the biaxial stress ratio B, σ_2, and the strength tensors is:

$$B^2F_{11}\sigma_2^2 + 2BF_{12}\sigma_2^2 + F_{22}\sigma_2^2 + BF_1\sigma_2 + F_2\sigma_2 = 1 \qquad (12)$$

F_{12} for a specified v_f is determined by solving equation (12) using the known values of F_1, F_2, F_{11}, F_{22}, B and the experimentally determined

value of $\sigma_2 = \sigma_2$. The absolute scatter ΔF_{12} of such an experiment [3] can be computed and is found to be:

$$\Delta F_{12} = \frac{\Delta\sigma_2}{\sigma_2} \left(F_{11}B + 2F_{12} + \frac{F_{22}}{B} + \frac{F_1}{2\sigma_2} + \frac{F_2}{2B\sigma_2}\right) \tag{13}$$

Relative scatter of the experimental measurement $\Delta\sigma_2/\sigma_2$ was taken to be 10%. Numerical values of ΔF_{12} are tabulated (Table 1) and serve as the scatter band for each determination of F_{12} as shown in Fig. 6.

The individual experimentally observed values of F_{12} and the associated scatter band served as the basis for determining the functional dependency of F_{12} on v_f. Each experimental point was assigned a weighing factor proportional to the reciprocal of the square of ΔF_{12} for that observation. Linear regression analysis was then carried out to find the pair of straight lines which best fit the experimental data (best fit in sense of smallest root mean square error).

The resulting relationships were:

$$F_{12} = 37.78\ v_f - 17.98 \tag{14}$$

$$0\% \leq v_f \leq 51\%$$

$$F_{12} = -3.39\ v_f + 3.02 \tag{15}$$

$$51\% \leq v_f \leq 100\%$$

Assuming that the value of F_{12} lying on the line (Eq. 14 or 15) was the exact value of F_{12} a calculation was carried out to determine the biaxial stress ratio B which minimized ΔF_{12} for a given volume fraction. Based on this value the resulting stress σ_2 which satisfied the failure criterion Eq. (12) was determined.

Propagation of error theory then dictates that the standard deviation in the calculated value of F_{12} is given by:

$$SD_{F_{12}}^2 = \left(\frac{\partial F_{12}}{\partial \sigma_2}\right)^2 SD_{F_2}^2 + \left(\frac{\partial F_{12}}{\partial F_{11}}\right)^2 SD_{F_{11}}^2 + \left(\frac{\partial F_{12}}{\partial F_{22}}\right)^2 SD_{F_{22}}^2 + \left(\frac{\partial F_{12}}{\partial F_1}\right)^2 SD_{F_1}^2 + \left(\frac{\partial F_{12}}{\partial F_2}\right)^2 SD_{F_2}^2 \quad (16)$$

where cross terms and any error in B have been neglected.

Computation of the various partial derivatives and substitution for the known standard derivations in Eq. (16) allows the standard deviation of F_{12} to be determined. The result is depicted in Fig. 7 as a pair of dashed lines.

Discussion

Tensor-Polynomial Criterion

The utility of the results presented lies in the ability to predict failure in the entire σ_1-σ_2 plane for any v_f based upon the functional dependency of the five strength tensors which characterize the tensor polynomial failure criterion. Fig. 8 dpicts predicted failure curves with four different volume fractions represented in the range $40\% \leq v_f \leq 70\%$. Clearly differences between the various predictions are not negligible. Table 2 lists the variation in failure surface center, inclination, and semi-axes as the volume fraction is varied. Center shift and increase in semi-axes length are the predominate characterizing parameters.

Comparison to Maximum Strain in Stress Space

In current engineering applications the other commonly used failure criterion is maximum strain which is usually presented in stress space.

Wu [9] treats the maximum strain criterion in stress stress and shows that it assumes the form of a parallelogram whose sides pass through the longitudinal tensile strength point with slope (S_{11}/S_{12}) and through the transverse tensile strength point with slope (S_{12}/S_{22}). Maximum strain assumes the above form via a mapping from strain space to stress space through the generalized linear Hooke's law $(\varepsilon_i = S_{i\,j}\,\sigma_j)$.

Fig. 9 and Fig. 10 depict the tensor polynomial criterion and the maximum strain criterion in relation to several experimentally determined combined stress failure points for v_f = 70% and 59% respectively. Clearly, the maximum strain criterion correlates observed failure in a very poor fashion. Agreement with the tensor polynomial criterion is quite good. The most objectionable feature of the maximum strain criterion in stress space is that it incorrectly predicts that a loading in the transverse direction will induce a compressive (Poisson's) failure in the longitudinal direction at a stress which is less than the observed failure stress.

Perhaps, the assumed linearity in generalized Hooke's law used to express maximum strain in stress space is unwarranted. A more just evaluation of the maximum strain-criterion must be carried out in strain-space.

Maximum Strain in Strain Space

Fig. 11 shows the maximum strain criterion in quadrants one and four of strain space. The values of ultimate strain needed to construct the failure envelope were experimentally determined in [6]. Experimentally determined complex stress failure points are shown for v_f = 70% in (Fig. 11a) and for v_f = 59% in (Fig. 11b). Maximum strain adequately

predicts failure in strain space. The fact that the experimentally determined stress strain curve under biaxial loading markedly depart from linearity accounts for the discrepancy observed in stress space. Assuming a linear generalized Hooke's law to express maximum strain in stress space can lead to gross error.

Conclusion

The dependency of composite strength under combined normal stress has been experimentally determined as fiber content was varied over the range $40\% \leq v_f \leq 75\%$. Failure predictions of the tensor polynomial criterion agree well with experimental data in stress space. The maximum strain criterion predicts a physically inadmissible failure envelope in stress space due to the assumed linear constitutive law. In strain space the maximum strain criterion agrees favorably with experimental observation.

Acknowledgment

This research was supported by the Advanced Research Projects Agency of the Department of Defense and was monitored by the Office of Naval Research under Contract No. N00014-67-C-0218.

References

1. Tsai, S. W. and Wu, E. M., "A General Theory of Strength for Anisotropic Materials", J. Comp. Matls., Vol. 5, pp. 58-80, 1971.

2. Collins, B. R. and Crane, R. L., "A Graphical Representation of the Failure Surface of a Composite", J. Comp. Matls., Vol. 5, pp. 408-413, 1971.

3. Wu, E. M., "Optimal Experimental Measurements of Anisotropic Failure Failure Tensors", J. Comp. Matls., Vol. 6, pp. 472-489, 1972.

4. Eisenhart, L. P., Transformations of Surfaces, 2nd ed. New York, Chelsea Pub. Co., 1962.

5. Lavengood, R. E. and Ishai, O., "The Mechanical Performance of Cross-Plied Composites", Polymer Engineering and Sci., Vol. 11, No. 3, pp. 226- , 1971.

6. Michno, M. J., Jr. and Shea, F. J., "Tensile (Compressive) Properties of Glass-Epoxy Composites as a Function of Volume Fraction", Monsanto/Washington University Assoc. HPC 73-163, 1973.

7. Young, H. D., Statistical Treatment of Experimental Data, McGraw-Hill, 1962.

8. Lavengood, R. E. and Michno, J. J., Jr., "Composite Shear Strength-Tube Torsion vs. Short Beam Shear", Monsanto/Washington University Assoc. HPC 73-155, 1973.

9. Wu, E. M. "Phenomenological Anisotropic Failure Criterion", in Treatise on Composite Materials, Vol. Ed. Sendeckyj, G., Series Ed. Broutman, L. and Crock, R., Academic Press, 1974.

Table 1

Results of biaxial normal stress experiments to determine F_{12}.

v_f(%)	$B = \sigma_1/\sigma_2$	σ_2(Ksi)	$F_{12} \times 10^{-4}(Ksi)^{-2}$	$\Delta F_{12} \times 10^{-4}(Ksi)^{-2}$
39.5	- 6.7	-13.2	- 0.8	1.5
42	- 8.6	-11.4	- 1.3	1.5
42.5	-11.8	- 8.2	- 3.1	1.9
43	-19.3	- 5.0	- 4.9	2.8
43	-27.9	- 3.8	- 3.2	3.3
44	-60.3	- 1.8	- 2.5	6.1
46.5	- 8.1	- 9.8	- 5.4	2.0
48	-33.6	- 3.8	- 0.2	2.8
49	- 6.7	-15.6	- 0.3	1.2
50	- 3.1	-29.6	+ 4.5	0.9
51	- 9.1	-13.8	0.0	1.1
52.5	- 1.2	-26.1	+ 5.4	2.9
57	- 2.6	-25.5	+ 2.0	1.4
58	- 5.6	-24.2	+ 1.8	0.7
59	+16.6	+ 4.1	+ 7.6	2.9
60	- 2.5	-28.4	+ 3.0	1.2
66	- 4.8	-26.1	+ 1.4	0.7
67	- 8.1	-15.4	- 1.5	1.0
69	- 6.9	-23.2	+ 1.0	1.0
70	- 6.6	-24.2	+ 1.1	0.6
70	- 6.0	-23.5	+ 0.7	0.7
70	-10.2	-14.8	- 0.7	0.9
70.5	- 6.4	-17.9	- 1.4	1.0
72.5	- 8.0	-19.4	0.0	0.7
73	- 8.7	-19.8	+ 0.4	0.6
74	- 6.6	-23.5	+ 0.6	0.6
74.5	- 6.3	-21.6	- 0.1	0.7
75	- 5.9	-25.1	+ 0.7	0.6
76.5	- 6.5	-24.6	+ 0.7	0.6

Table 2

Parameters for σ_1-σ_2 failure curves vs v_f.

Fig. 8 Curve	v_f%	$F_{12} \times 10^{-4}$	Center σ_1, σ_2(Ksi)	Inclination wrt σ_1	Semi Axes (Ksi)
a	47.5	0.0	12.8, - 7.2	0	101.0, 12.0
b	40	-2.83	5.8, - 7.6	1 cw	95.3, 11.3
c	55	+1.16	38.6, -15.1	1/2 ccw	110.6, 12.7
d	70	+ .65	66.1, -16.7	5/12 ccw	126.8, 14.1

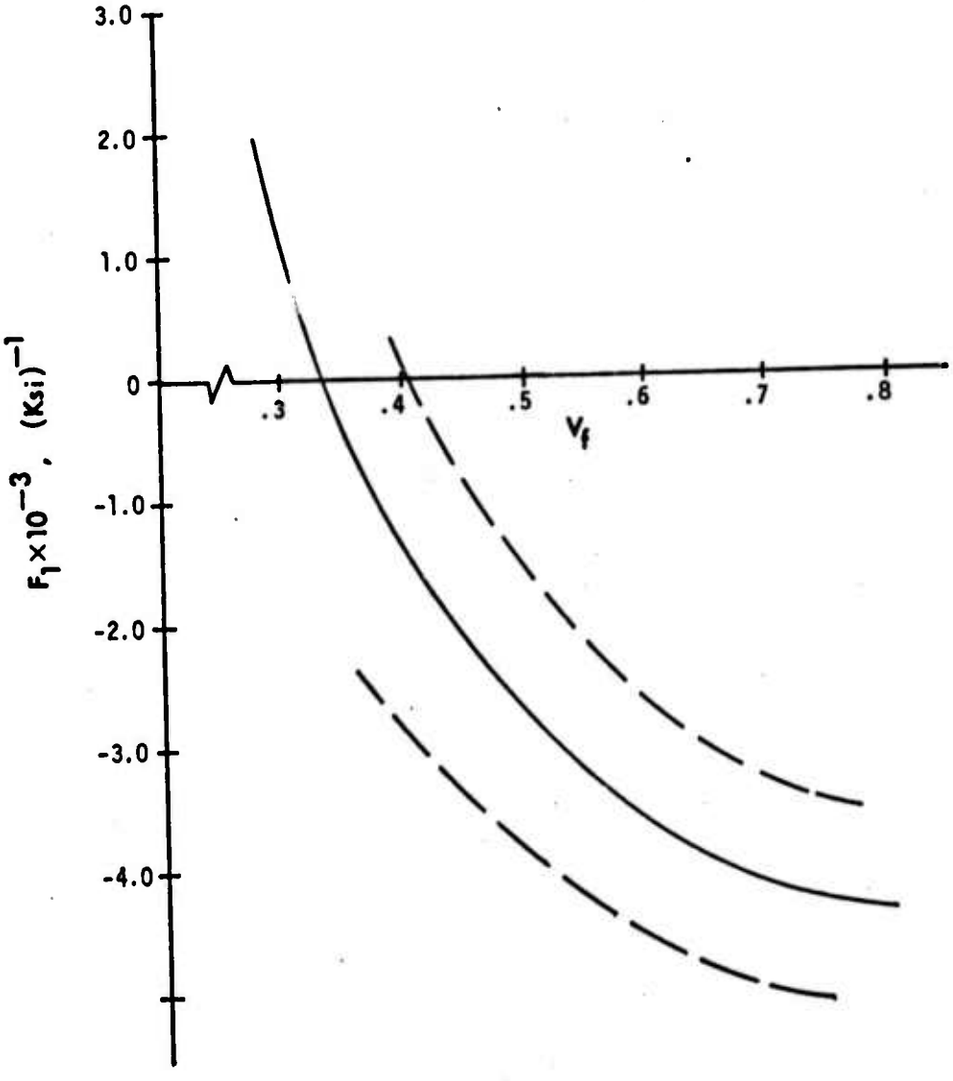

Figure 1. Second order longitudinal strength tensor, F_1 vs v_f.

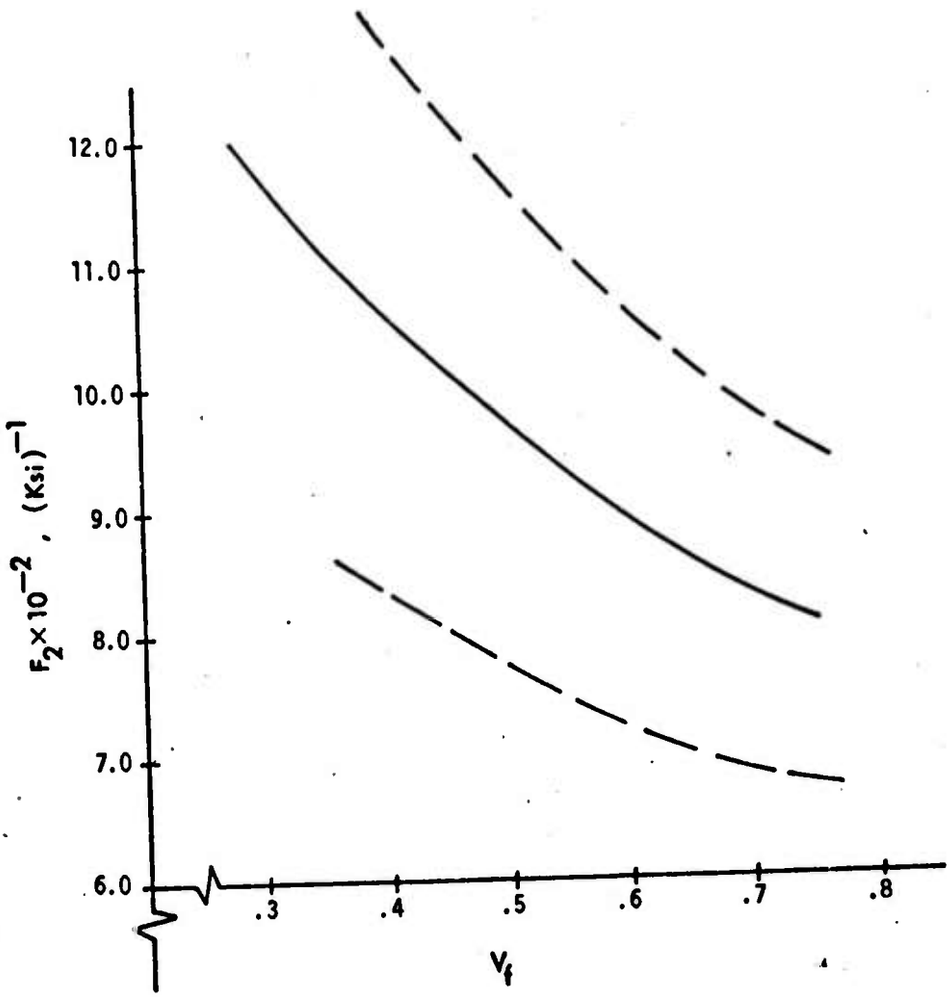

Figure 2. Second order transverse strength tensor, F_2 vs v_f.

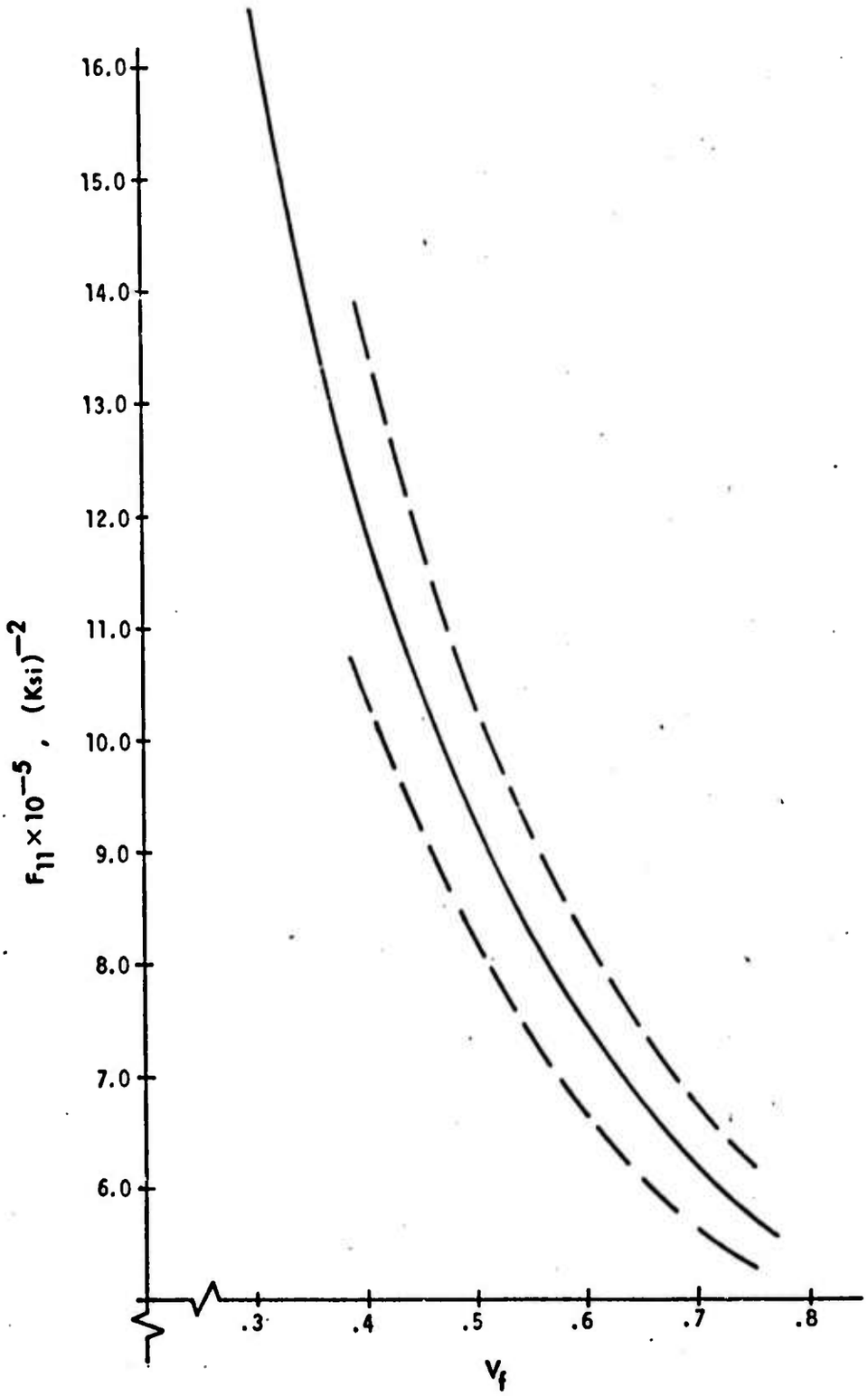

Figure 3. Fourth order longitudinal strength tensor, F_{11} vs v_f.

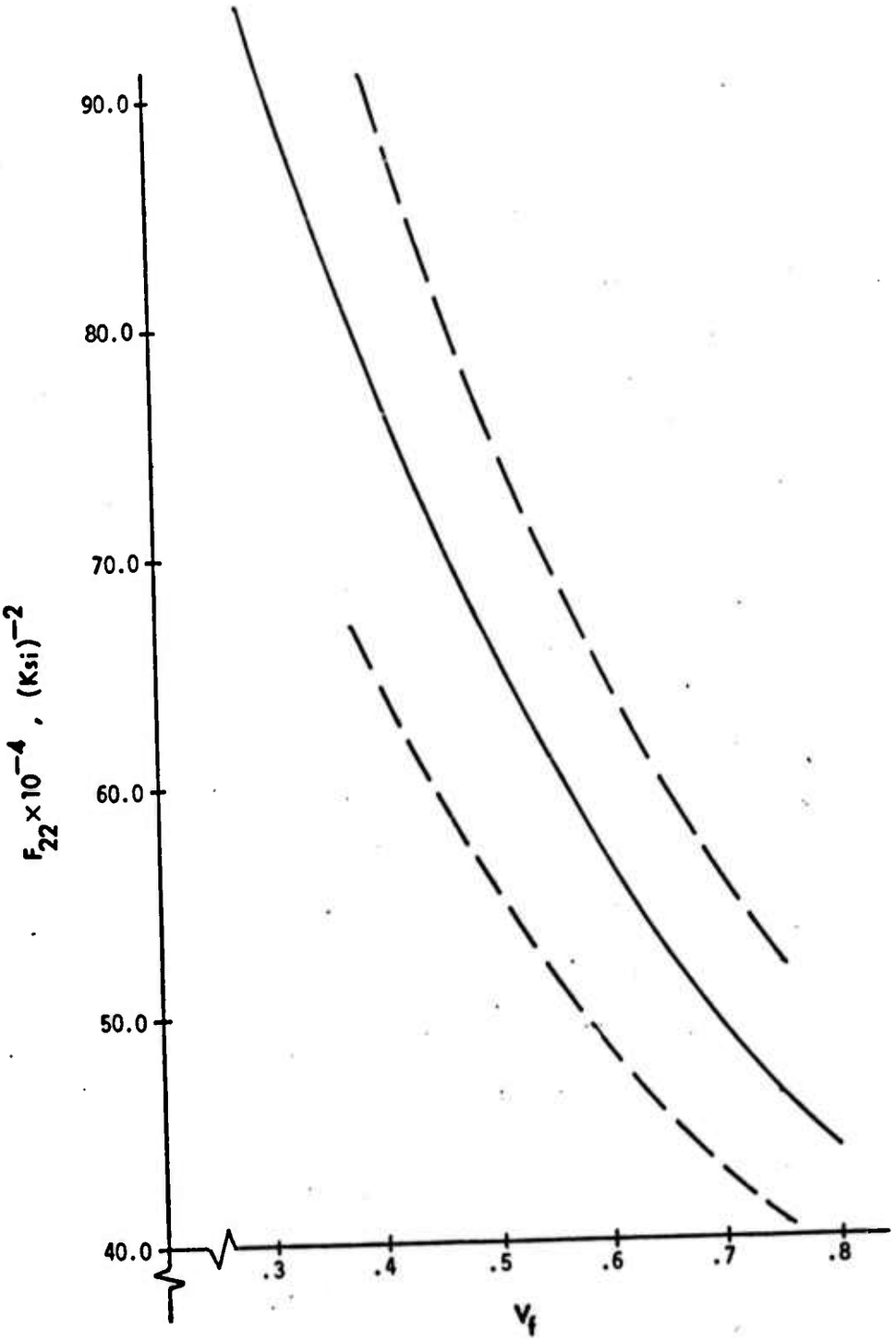

Figure 4. Fourth order transverse strength tensor, F_{22} vs v_f.

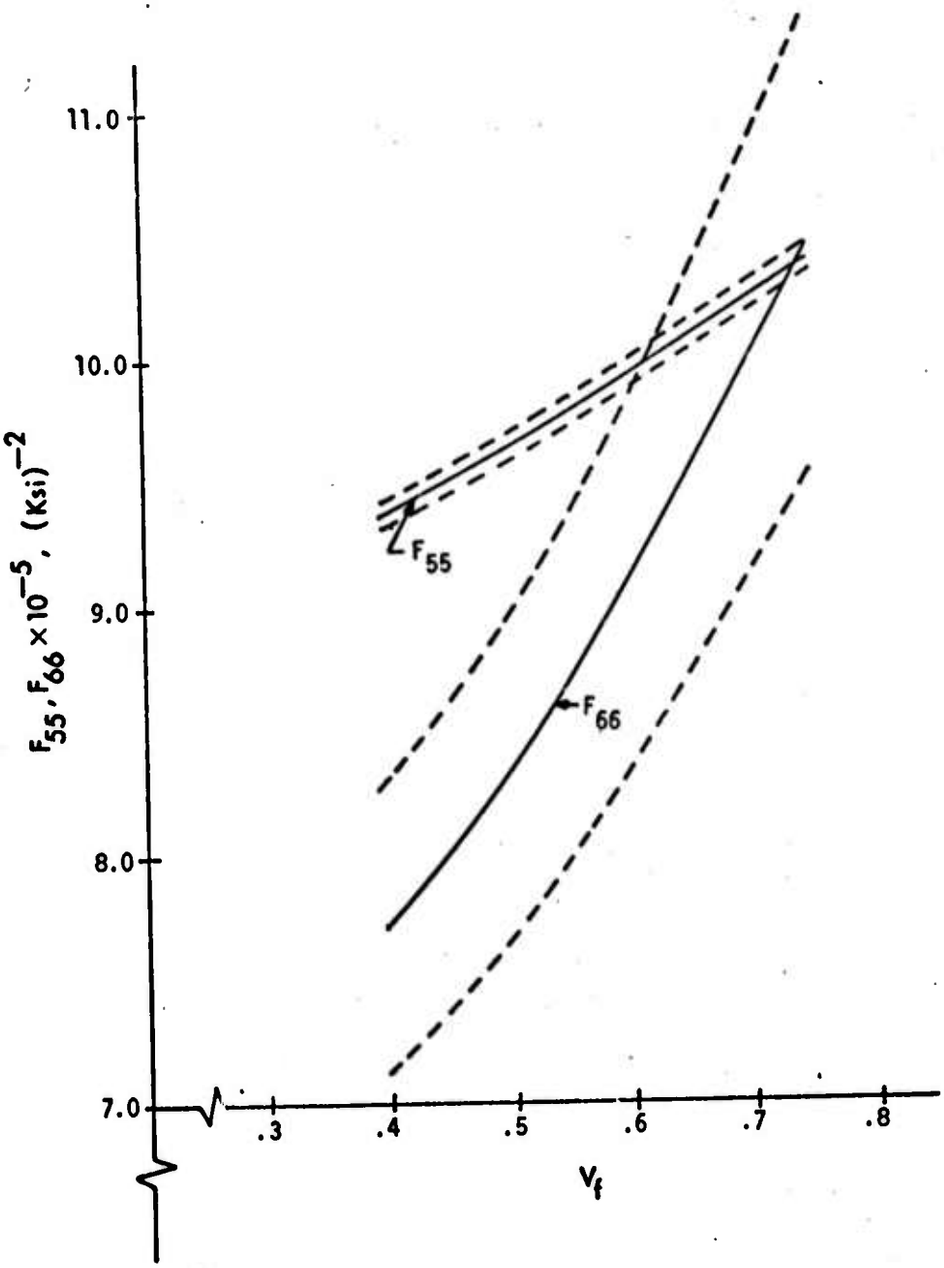

Figure 5. Fourth order shear strength tensors, F_{55}, F_{66} vs v_f.

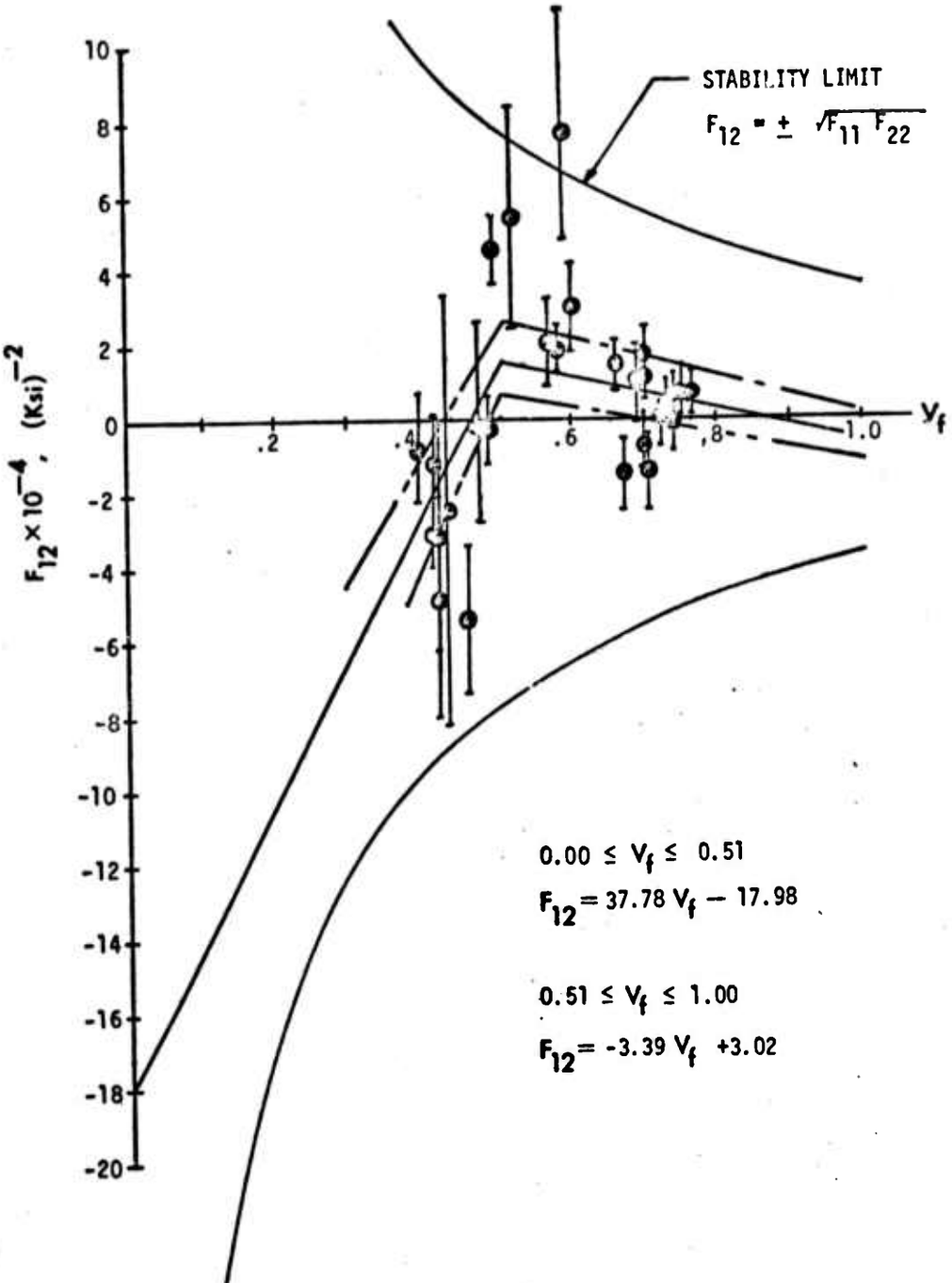

Figure 6. Normal stress interaction strength tensor, F_{12} vs v_f.

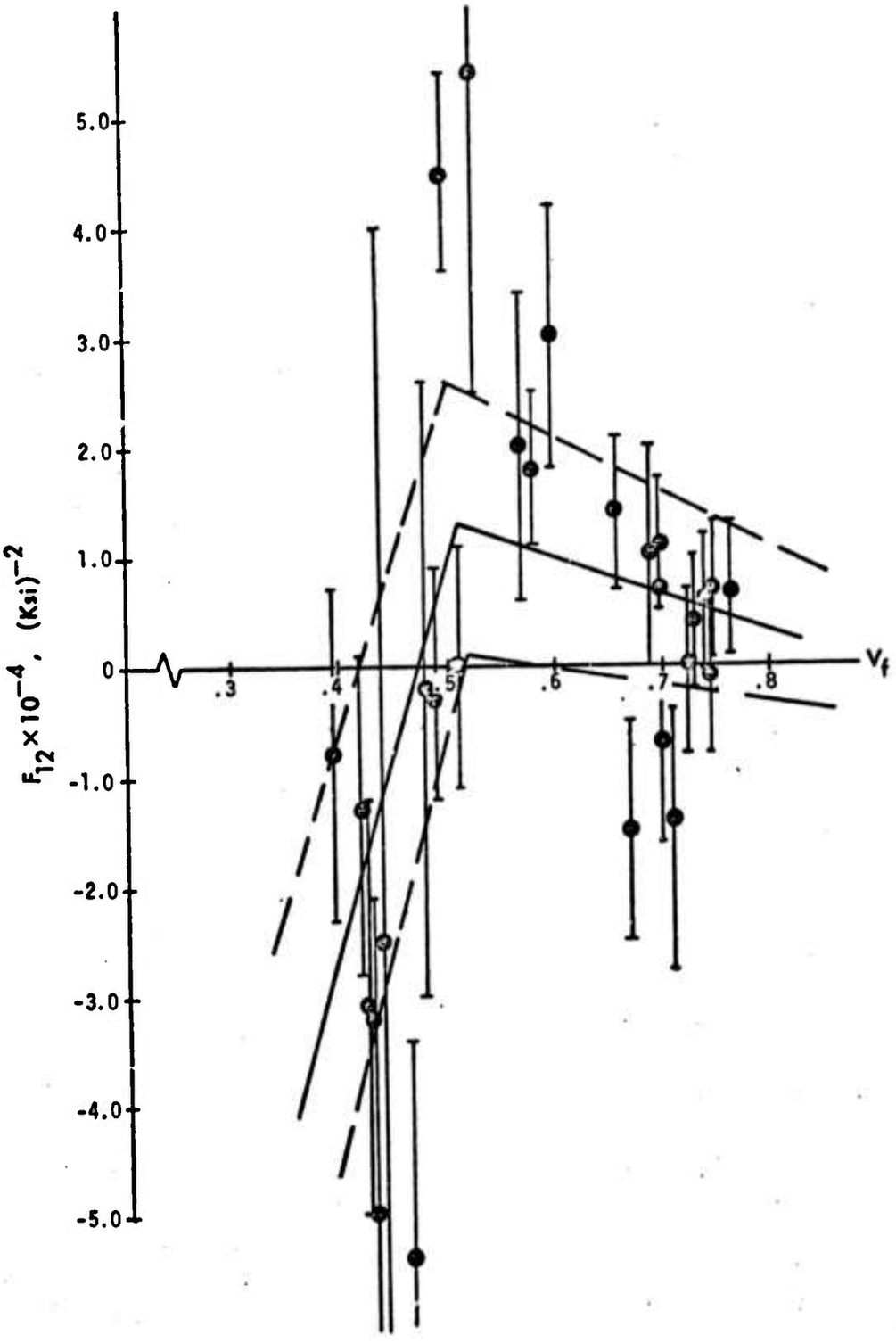

Figure 7. Standard deviation of F_{12} vs V_f.

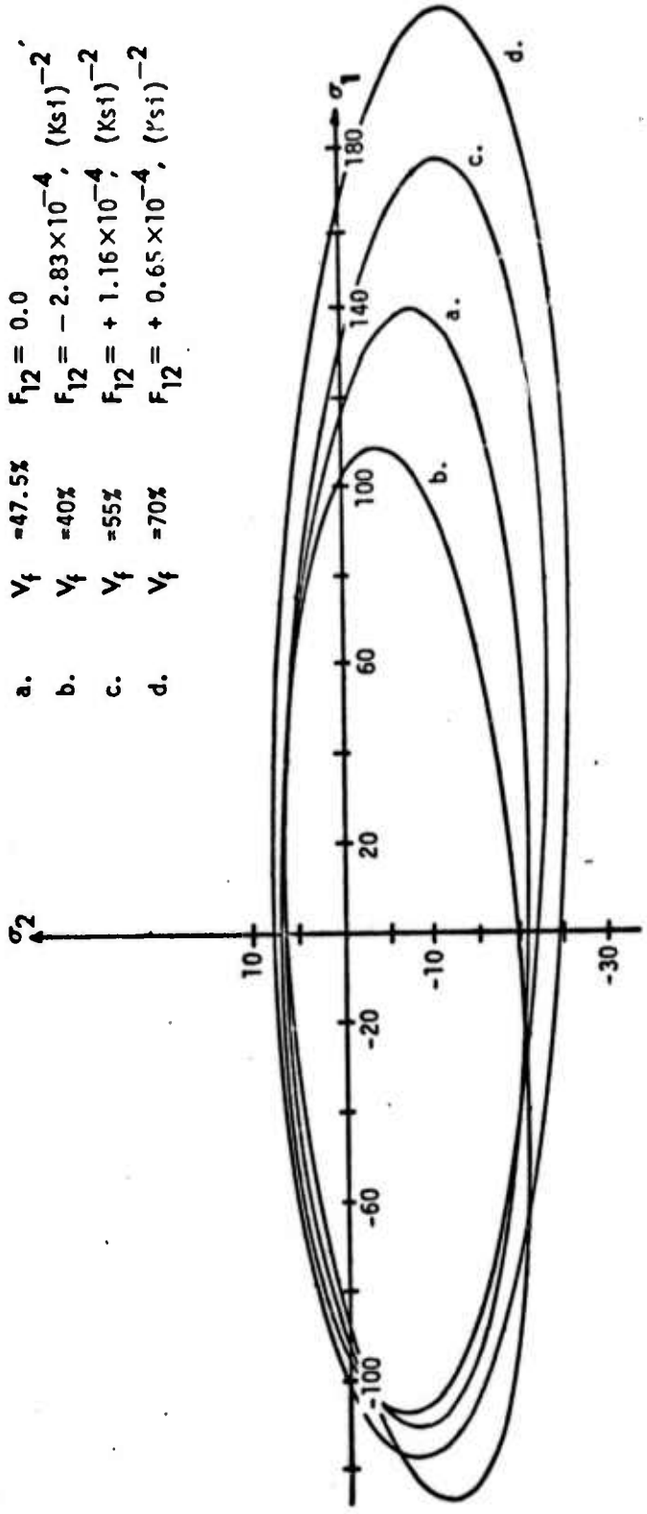

Figure 8. Predicted normal stress failure curves vs V_f.

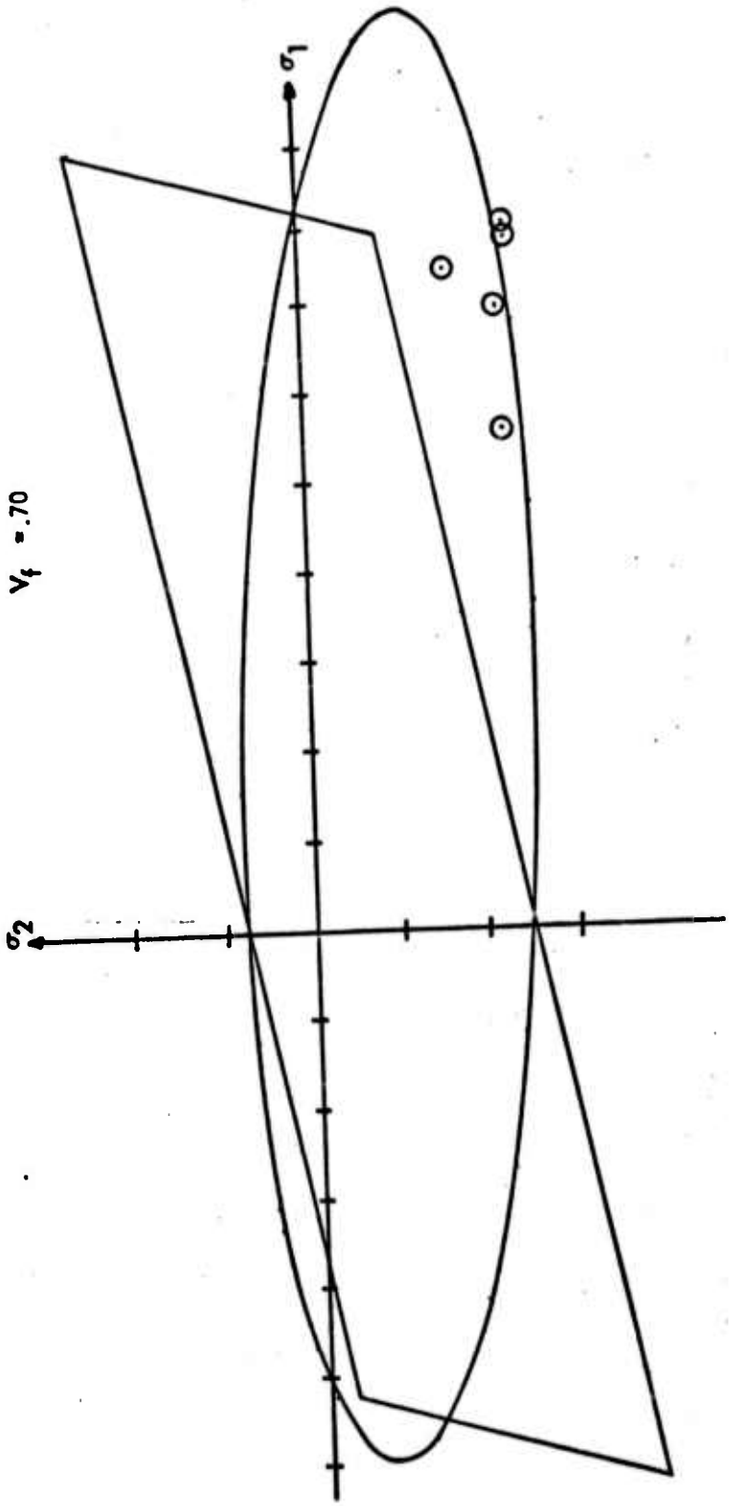

Figure 9. v_f = .70, experimental results vs Maximum Strain and Tensor Polynomial predictions in stress space.

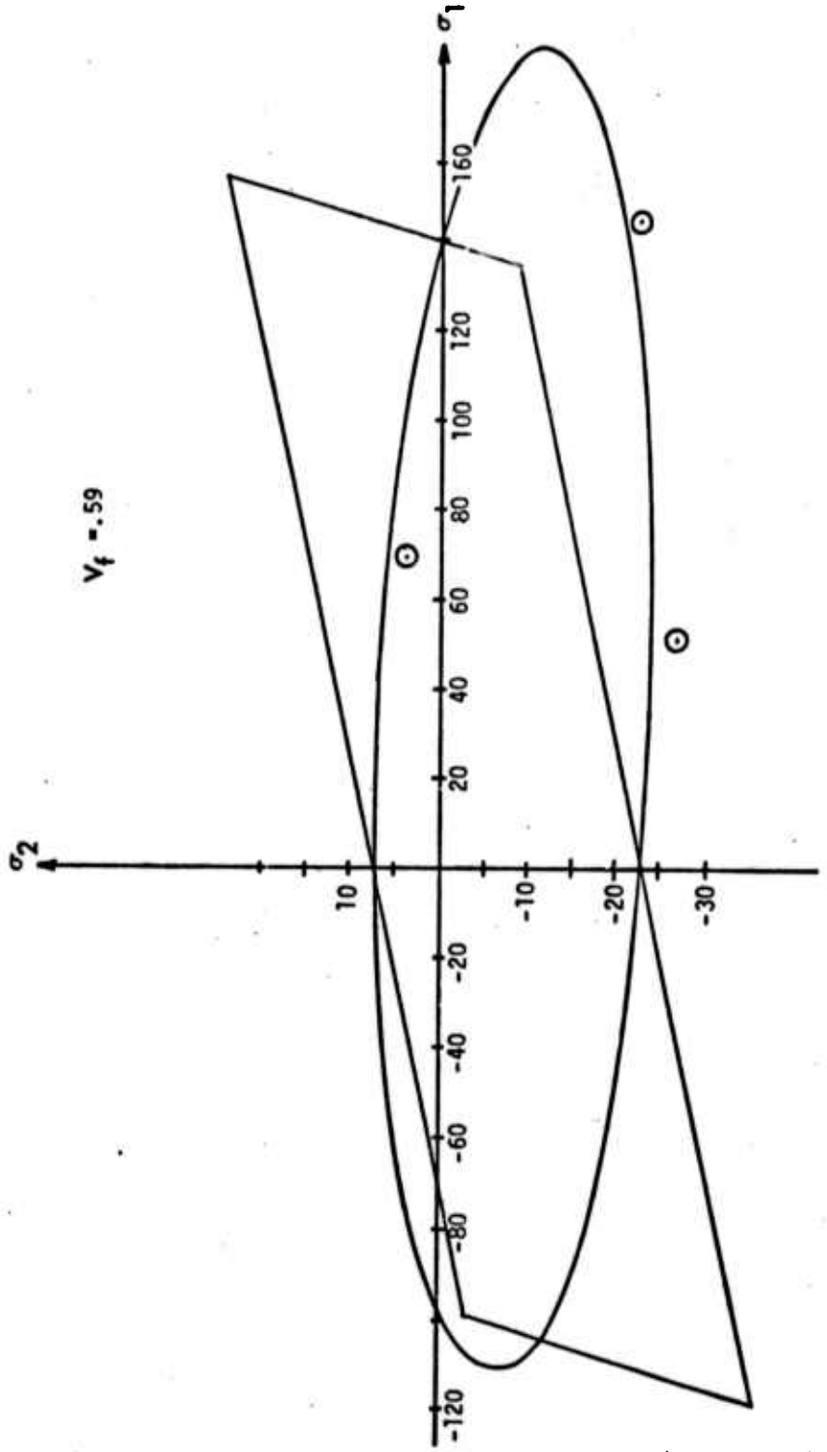

Figure 10. v_f = .59, experimental results vs Maximum Stain and Tensor Polynomial predictions in stress space.

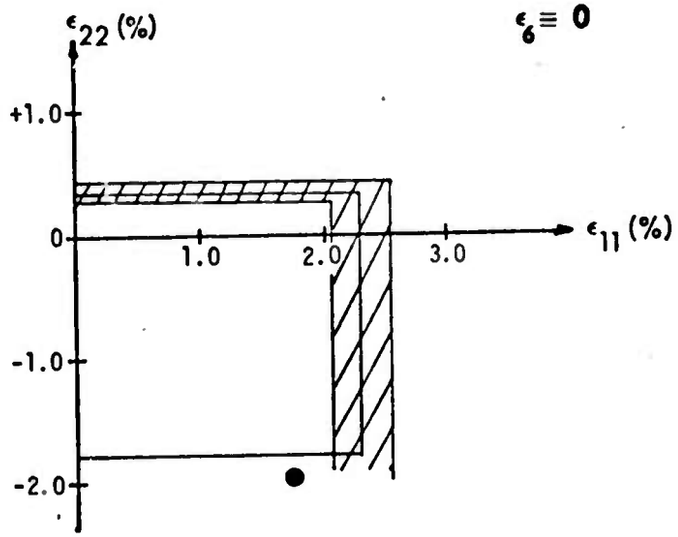

a) MAXIMUM STRAIN V_f = .70

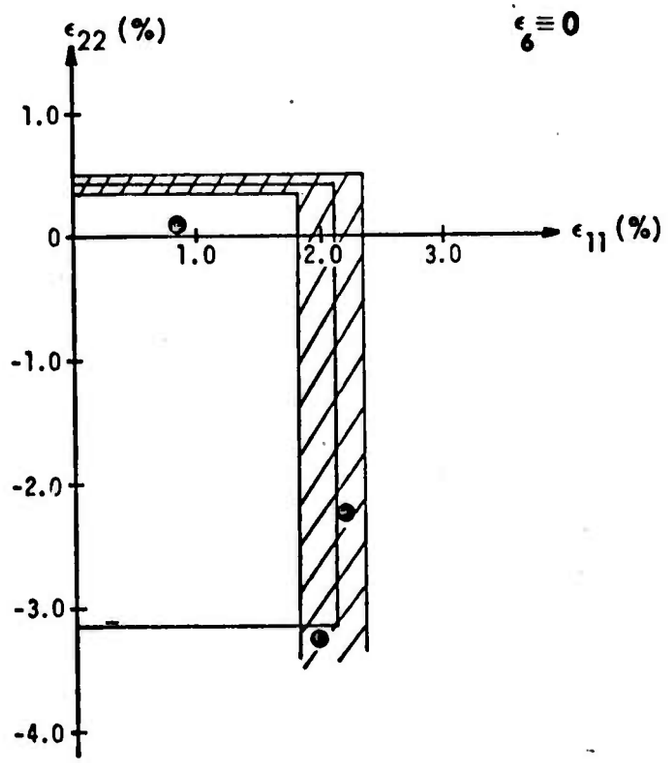

b) MAXIMUM STRAIN V_f = .59

Figure 11. Maximum strain vs experimental results in strain space.